Progress in PHOTOVOLTAICS

PROGRESS IN PHOTOVOLTAICS: RESEARCH AND APPLICATIONS
Prog. Photovolt: Res. Appl. 2013; **21**:1087–1094
Published online 9 May 2012 in Wiley Online Library (wileyonlinelibrary.com). DOI: 10.1002/pip.2210

RESEARCH ARTICLE

Basic aspects of the temperature coefficients of concentrator solar cell performance parameters

Avi Braun[1], Eugene A. Katz[1,2] and Jeffrey M. Gordon[1,3]*

[1] Department of Solar Energy and Environmental Physics, Jacob Blaustein Institutes for Desert Research, Ben-Gurion University of the Negev, Sede Boqer Campus 84990, Israel
[2] The Ilse Katz Institute for Nanoscale Science and Technology, Ben-Gurion University of the Negev, Beersheva 84105, Israel
[3] The Pearlstone Center for Aeronautical Engineering Studies, Department of Mechanical Engineering, Ben-Gurion University of the Negev, Beersheva 84105, Israel

ABSTRACT

The basis for the temperature dependence of the principal performance parameters of single and multi-junction concentrator solar cells is examined, focusing on the impact of bandgap and irradiance. The analysis of cells in the radiative limit establishes fundamental bounds. A quasi-empirical model yields predictions consistent with available data. A simple method for estimating the temperature coefficients of key performance parameters is identified. The degree to which the efficiency penalty associated with cell heating can be mitigated by high irradiance is also evaluated. Copyright © 2012 John Wiley & Sons, Ltd.

KEYWORDS
concentrator; solar cell; temperature coefficient; efficiency; bandgap; multi-junction

***Correspondence**
Jeffrey M. Gordon, Department of Solar Energy and Environmental Physics, Jacob Blaustein Institutes for Desert Research, Ben-Gurion University of the Negev, Sede Boqer Campus 84990, Israel.
E-mail: jeff@bgu.ac.il

Received 13 November 2011; Revised 9 January 2012; Accepted 5 March 2012

1. INTRODUCTION

Photovoltaic operating temperatures are commonly tens of degrees above the standard testing value of 25 °C for both flat-plate and concentrator systems. The associated efficiency reduction is non-negligible. Although the impact of temperature on efficiency has been studied—including experiments on single-junction [1–6] and multi-junction [6–11] cells—the data and theoretical underpinning for concentrator photovoltaics have not been extensive, especially on how the effect of temperature on cell performance changes with irradiance. Recent experiments showed that the magnitude of the efficiency penalty for cell heating decreases significantly with irradiance [6–8,12]—by as much as a factor of two at flux concentration values of order 10^3 suns [12]. This paper examines whether ultra-high irradiance could render the effect of cell heating negligible, or even beneficial.

Here, we investigate the basis for the effect of irradiance on the temperature dependence of the key cell performance parameters: short-circuit current density J_{sc}, open-circuit voltage V_{oc}, fill factor FF, and efficiency η. In so doing, we (i) identify and quantify the individual contributions to these temperature coefficients, (ii) establish fundamental bounds for their magnitude from the radiative limit, with an ideal external quantum efficiency (EQE), and (iii) develop a quasi-empirical model that affords satisfactory predictions compared with available data and obviates the need for extensive measurements at numerous irradiance levels. We proceed by portraying the analytic models, scrutinizing their predictions, and offering comparisons to available data.

2. ANALYTIC MODEL

2.1. Short-circuit current density

In single-junction cells, J_{sc} depends only on the input spectral photon flux density $f(E)$ (photons per unit time, per unit area, per unit energy) and the EQE. The temperature (T) dependence of J_{sc} then stems from that of the EQE:

$$J_{sc}(T) = q\int_0^\infty EQE(E,T)\cdot f(E)dE \qquad (1)$$

The ideal EQE is a step-function: zero for photon energies below the bandgap energy ($E < E_g$) and unity for $E > E_g$, for which

$$J_{sc}(T) = q \int_{Eg(T)}^{\infty} f(E)dE, \quad \frac{dJ_{sc}}{dT} = -q \cdot f(E_g)\frac{dE_g}{dT} \quad (2)$$

where q is the elementary charge. Equation 2 is valid provided that J_{sc} is proportional to irradiance. (J_{sc} may not be proportional to irradiance in cells with large series resistance losses [13], or irradiance values so high that the immense carrier densities reduce optical absorption [14].)

For common solar cell materials (e.g., Si, GaAs, Ge, GaSb, GaInP), dE_g/dT is well approximated by $-(2\beta + T)\alpha T/(T+\beta)^2$ (α and β are empirical parameters) and ranges from -0.26 to -0.55 meV/K, with a temperature dependence of only a few percent from 0 to 100 °C [15–18]. Hence, dJ_{sc}/dT is a positive linear function of the photon flux density in the vicinity of E_g (Eq. 2).

The analysis is complicated when the sub-cells in multijunction (MJ) solar cells are connected in series, wherein J_{sc}^{MJ} is controlled by the current-limiting sub-cell [19]. Cell heating may increase current in the current-limiting sub-cell (due to enhanced long-wavelength absorption) but is counterbalanced by the corresponding current increase in the top sub-cell (unless the current-limiting sub-cell is the top sub-cell, in which case the temperature dependence of J_{sc} is simply that of a single-junction cell with the same bandgap as that of the top sub-cell). Then dJ_{sc}^{MJ}/dT is the difference between the temperature coefficient of the limiting sub-cell $d{J_{sc}}^{i}/dT$ and the one above it is dJ_{sc}^{i-1}/dT:

$$J^{MJ}{}_{sc}(T) = J^{i}{}_{sc}(T) = q \int_{Eg^{i}(T)}^{Eg^{i-1}(T)} f(E)dE,$$
$$\frac{dJ^{MJ}{}_{sc}}{dT} = q\left[f\left(E_g^{i-1}\right)\frac{dE^{i-1}{}_g}{dT} - f(E^{i}{}_g)\frac{dE^{i}{}_g}{dT}\right]. \quad (3)$$

One qualification is that the sub-cell that limits overall cell current can shift when the J_{sc} values of sub-cells are nearly the same, because of either (i) a difference in the temperature coefficient of the sub-cell bandgaps, or (ii) the impact of the input spectral distribution especially at the low and high-wavelength extremes of the sub-cell spectral response curves [9–11]. That notwithstanding, Eq. 3 remains valid for a given cell temperature.

2.2. Open-circuit voltage

The dependence of V_{oc} on T and flux concentration X is implicit in the basic relation

$$V_{oc} = (nkT/q)\ln(J_{sc}/J_0) \quad (4)$$

where n denotes the diode quality factor, k is Boltzmann's constant, and J_0 is the saturation current density. The dependence of V_{oc} on T and X is then subsumed in

$$\begin{aligned} V_{oc}(T,X) &= (nkT/q)\ln\left(X \cdot J_{sc,1\ sun}(T)/J_0(T)\right) \\ &= V_{oc,1\ sun}(T) + \frac{nkT}{q}\ln(X) \quad (a) \\ \frac{dV_{oc}(T,X)}{dT} &= \left.\frac{dV_{oc}(T)}{dT}\right|_{1\ sun} + \frac{nk}{q}\ln(X) \quad (b) \end{aligned} \quad (5)$$

In the radiative limit, $n = 1$ (per junction) and [20]

$$\begin{aligned} J_0 &= \frac{2\pi q}{h^3c^2}\int_{E_g}^{\infty}\frac{E^2}{e^{E/kT}-1}dE \\ &\approx \frac{2\pi qk^3}{h^3c^2}T^3 \cdot \left(\left(E_g/kT\right)^2 + 2E_g/kT + 2\right) \cdot e^{-E_g/kT} \\ &\approx \frac{2\pi qk}{h^3c^2}T \cdot {E_g}^2 \cdot e^{-E_g/kT} \end{aligned} \quad (6)$$

where c is the speed of light and h is Planck's constant. (The approximation $e^{E/kT} >> 1$ in the denominator of the integrand is accurate to better than one part in 10^8 for $E_g > 0.5$ eV.) With the differentiation of Eq. (5a) with respect to T and introduction of Eq. 6, the temperature coefficient of V_{oc} in the radiative limit is

$$\begin{aligned} \frac{dV_{oc}(T,X)}{dT} = &\frac{V_{oc,1\ sun}(T) + \frac{kT}{q}\ln(X) - \frac{E_g(T)}{q}}{T} \\ &-\frac{k}{q}\left(1 + 2\frac{d\ln E_g(T)}{d\ln T}\right) + \frac{1}{q}\frac{dE_g(T)}{dT} \\ &+\frac{k}{q}\frac{d\ln J_{sc,1\ sun}(T)}{d\ln T} \end{aligned} \quad (7)$$

In contrast to the radiative limit, the quasi-empirical approach provides a realistic estimate (rather than just a lower bound—*vide infra*) for the temperature coefficient of V_{oc} that can be compared with measured values. Three assumptions distinguish the quasi-empirical approach from the radiative limit. First, the reverse saturation current density J_0 is taken to be proportional to the square of the intrinsic carrier concentration [15]

$$J_0 \propto T^3 e^{-E_g/kT} \quad (8)$$

(as distinct from Eq. (6) for the radiative limit). Second, in contrast to the radiative limit, where V_{oc} is calculated from Eqs. 2, 4 and 6, the quasi-empirical model invokes

$$V_{oc} \approx E_g/q - 0.44\ \text{V} \quad (9)$$

at one sun, on the basis of the measurements from high-efficiency cells, spanning a wide range of E_g [21]. Third, the diode quality factor n is not necessarily equal to 1 (although in the calculations that follow, unless otherwise stated explicitly, the approximation $n \approx 1$ is used on the basis of the observed high-irradiance behavior of high-quality concentrator cells). Moreover, there are no adjustable parameters in the quasi-empirical approach.

Differentiating Eq. 5a with respect to T and introducing Eq. 8, one obtains the temperature coefficient of V_{oc} for the quasi-empirical model [8] (which differs non-negligibly from the corresponding result in the radiative limit, Eq. 7):

$$\frac{dV_{oc}(T,X)}{dT} = \frac{V_{oc,1\ sun}(T) + \frac{nkT}{q}\ln(X) - n\frac{E_g(T)}{q}}{T} - \frac{3nk}{q} + \frac{n}{q}\frac{dE_g(T)}{dT} + \frac{nk}{q}\frac{d\ln J_{sc,1\ sun}(T)}{d\ln T}. \tag{10}$$

Invariably, dV_{oc}/dT is negative because of the dominance of the first three terms on the right-hand side of Eqs. 7 and 10 (recall that $nE_g > qV_{oc}$ and $dE_g/dT < 0$). The radiative limit corresponds to the highest possible V_{oc} and hence sets a *lower* bound for the *magnitude* of dV_{oc}/dT. In addition, since V_{oc} increases with irradiance, the penalty for cell heating diminishes as flux concentration increases.

Equations 5, 7 and 10 indicate that one can estimate dV_{oc}/dT at high irradiance from measuring it at a single irradiance value, that is, one sun (provided n is known), thus obviating the need for measurements at every irradiance value. In instances where n changes with irradiance X [12,22], Eqs. 5 and 10 require piecewise analysis (with respect to $n(X)$). However, to find dV_{oc}/dT as function of X, one needs to only measure $V_{oc}(X)$ (and not $dV_{oc}/dT(X)$). It might also be noted that the method for estimating $dV_{oc}/dT(X)$ from (i) a single measurement of dV_{oc}/dT and (ii) $n(X)$ (Eq. 12), is not contingent upon the modeling introduced here.

Equations 5, 7 and 10 are also valid for serially connected sub-cells because V_{oc} and dV_{oc}/dT are then the sum of the contributions from the individual sub-cells:

$$V_{oc}{}^{MJ}(X) = \sum_i V_{oc,i} = \sum_i V_{oc,i,1\ sun} + \frac{kT\sum_i n_i}{q}\ln(X) \tag{11}$$

$$\left.\frac{dV_{oc}}{dT}\right|_X^{MJ} = \sum_i\left[\left.\frac{dV_{oc}{}^i}{dT}\right|_{1\ sun} + \frac{n^i k}{q}\ln(X)\right] = \left.\frac{dV_{oc}{}^{MJ}}{dT}\right|_{1\ sun} + \frac{n^{MJ}k}{q}\ln(X) \tag{12}$$

where n^{MJ} is the effective diode quality factor of the multi-junction cell. The validity of Eqs. 11, 12 at concentration levels up to ~10^4 suns was demonstrated in [12]. (One caveat is that at inordinately high irradiance values, where the quasi-Fermi levels are within the valence or conduction band—namely, when V_{oc} approaches E_g/q—cell absorption is reduced and $V_{oc}(T,X) \rightarrow E_g(T)/q$ [14] in lieu of Eq. 5a.)

2.3. Fill factor

For negligible series resistance losses (and provided bandgap values satisfy $E_g > 0.5$ eV for the radiative-limit case and $E_g > 0.65$ eV for the quasi-empirical model), the current density and voltage at maximum power point (J_{MP} and V_{MP}, respectively) are well approximated as [23]

$$V_{MP} = V_{oc} - \frac{nkT}{q}\ln\left(V_{MP}\frac{q}{nkT}+1\right) \approx V_{oc} - \frac{nkT}{q}\ln\left(V_{oc}\frac{q}{nkT}+1\right) \tag{13}$$

$$J_{MP} = J_{sc} - J_0\left(e^{\left(\frac{qV_{MP}}{nkT}\right)} - 1\right) \approx J_{sc} - J_0\left\{\frac{e^{\left(\frac{qV_{oc}}{nkT}\right)}}{\left(\frac{qV_{oc}}{nkT}+1\right)} - 1\right\} \approx J_{sc} - \frac{J_0 e^{\left(\frac{qV_{oc}}{nkT}\right)}}{\left(\frac{qV_{oc}}{nkT}+1\right)} \tag{14}$$

(In Eq. 13, V_{MP} in the logarithm has been approximated by V_{oc}, and in Eq. 14, the approximation $\exp(qV_{oc}/nkT) >> qV_{oc}/nkT$ has been used.) One can then express FF and dFF/dT of single-junction cells as

$$FF(T,X) \approx \frac{V_{oc,1\ sun}\frac{q}{nkT} + \ln(X) - \ln\left(V_{oc,1\ sun}\frac{q}{nkT} + \ln(X) + 1\right)}{V_{oc,1\ sun}\frac{q}{nkT} + \ln(X) + 1} \tag{15}$$

$$\frac{dFF(T,X)}{dT} \approx \frac{\ln\left(V_{oc,1\ sun}(T)\frac{q}{nkT} + \ln(X) + 1\right)\left(\frac{dV_{oc,1\ sun}(T)}{dT}\frac{q}{nkT} - V_{oc,1\ sun}(T)\frac{q}{nkT^2}\right)}{\left(V_{oc,1\ sun}(T)\frac{q}{nkT} + \ln X + 1\right)^2} \tag{16}$$

Hence, dFF/dT is negative, with a magnitude that (i) decreases as V_{oc} and X increase and (ii) is minimal in the radiative limit. Beyond the aim of establishing results for the ideal limit, the analysis for FF was also restricted to zero series resistance because there is no universal generalization for non-negligible R_s. The observed trend, however, is for the magnitude of dFF/dT to increase with R_s [9]. In serially connected multi-junction cells, FF and dFF/dT change with the degree of current mismatch [9] and cannot be expressed analytically. (In exceptional cases where cells experience tunnel-diode transitions or suffer from Schottky contacts, dFF/dT can deviate significantly from Eq. 16 and may even become positive—not addressed here.)

3. RESULTS AND DISCUSSION

3.1. Short-circuit current density

The relative temperature coefficient $d\ln(J_{sc})/dT$ was calculated as a function of E_g for the AM1.5 d (ASTM G173-03) spectrum, $T = 25$ °C (conditions that pertain to all calculations and data are noted in the succeeding paragraphs), an ideal *EQE*, and dE_g/dT values of −0.26 and −0.46 meV/K (corresponding to Si and GaAs, respectively)—plotted in Figure 1 together with experimental results for a variety of single-junction cells. (The local minima in Figure 1 reflect the atmospheric absorption lines in the input spectral photon flux.) Consistent with corresponding experimental results, the predicted $d\ln(J_{sc})/dT$ increases with E_g because of lower photo-generated currents in high-E_g cells: from ~0.0001 K^{-1} for low-E_g materials with $dE_g/dT = -0.26$ meV/K, to 0.001 K^{-1} for high-E_g junctions with $dE_g/dT = -0.46$ meV/K. The modest discrepancies are attributable to the non-ideal *EQE* curves of realistic devices. Varying T by as much as 30 K turns out to have a basically negligible effect on $d\ln(J_{sc})/dT$.

3.2. Open-circuit voltage

Calculations of $d\ln(V_{oc})/dT$ as a function of E_g are presented in Figure 2 and are compared with experimental data, with both displaying the same trend: a decrease in $|d\ln(V_{oc})/dT|$ with E_g (due to a higher V_{oc}). The measured penalty for increased temperature is close to the values calculated using Eqs. 9–10 and, as expected, larger in magnitude than the basic lower bounds calculated for ideal cells in the radiative limit. The differences between the radiative limit and the quasi-empirical model decrease as E_g increases because of non-idealities (i.e., non-radiative losses) being most pronounced at low E_g.

To estimate the sensitivity of our calculations to cell temperature, we recalculated dV_{oc}/dT at 80 °C and found a change of only 3% relative to the value at 25 °C, both in the radiative-limit and with the quasi-empirical approach, in agreement with experimental measurements [12].

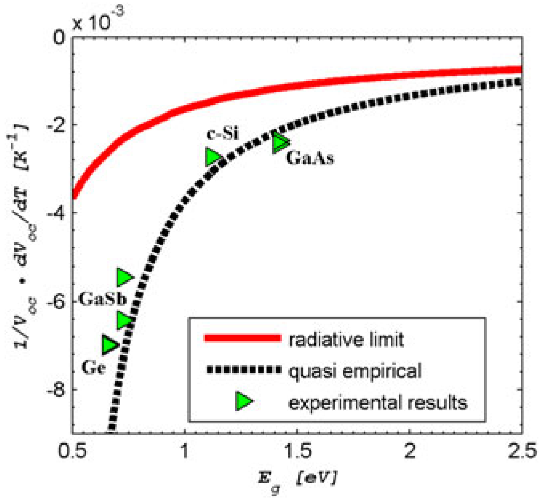

Figure 2. The relative temperature coefficient of V_{oc} as a function of E_g, at one sun, in the radiative limit and with the quasi-empirical model (due to the insensitivity of these results to dE_g/dT, an average value of −0.36 meV/K was used), along with corresponding data for single-junction cells (solid triangles) comprising the materials listed in Figure 1 [6,24].

Figure 3 demonstrates the impact of flux concentration on the magnitude of the temperature coefficient of V_{oc}. For example, for the $E_g = 1.0$ eV cell, when irradiance is increased from 1 to 10^4 suns, the magnitudes of dV_{oc}/dT and $d\ln(V_{oc})/dT$ decrease by factors of 3 and 4, respectively.

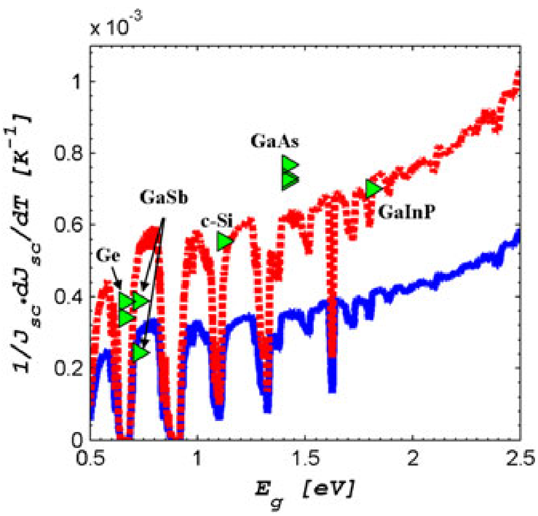

Figure 1. $d\ln(J_{sc})/dT$ calculated for materials with $dE_g/dT = -0.26$ (solid curve) and −0.46 meV/K (dashed curve). The solid triangles represent the corresponding measured values of single-junction cells, at one sun, for Ge ($E_g = 0.66$ eV), GaSb (0.726 eV), c-Si (1.12 eV), GaAs (1.42 eV) and GaInP (1.86 eV) [6,10,24].

3.3. Fill factor

The effects of irradiance and E_g on the temperature coefficient of *FF* were calculated using Eqs. 15–16 and were compared with experimental data (Figure 4). $d\ln(FF)/dT$ is negative, with a magnitude that decreases with both irradiance and E_g. Quasi-empirical model predictions are consistent with the one-sun data, including lower-magnitude temperature coefficients at higher E_g.

3.4. Efficiency

$d\ln(\eta)/dT$ is the sum of the corresponding contributions of the relative temperature coefficients of J_{sc}, V_{oc}, and *FF*, the magnitudes of which vary differently with E_g (Figure 5). While the magnitude of the negative contributions of V_{oc} and *FF* diminish as E_g increases, the positive contribution from J_{sc} increases, so that, for ideal cells, $d\ln(\eta)/dT$ is essentially zero at $E_g > 2.5$ eV. The quasi-empirical results agree with experimental measurements of $d\ln(\eta)/dT$, with magnitudes that noticeably exceed the basic lower bound of the radiative limit.

Prog. Photovolt: Res. Appl. 2013; **21**:1087–1094 © 2012 John Wiley & Sons, Ltd.
DOI: 10.1002/pip

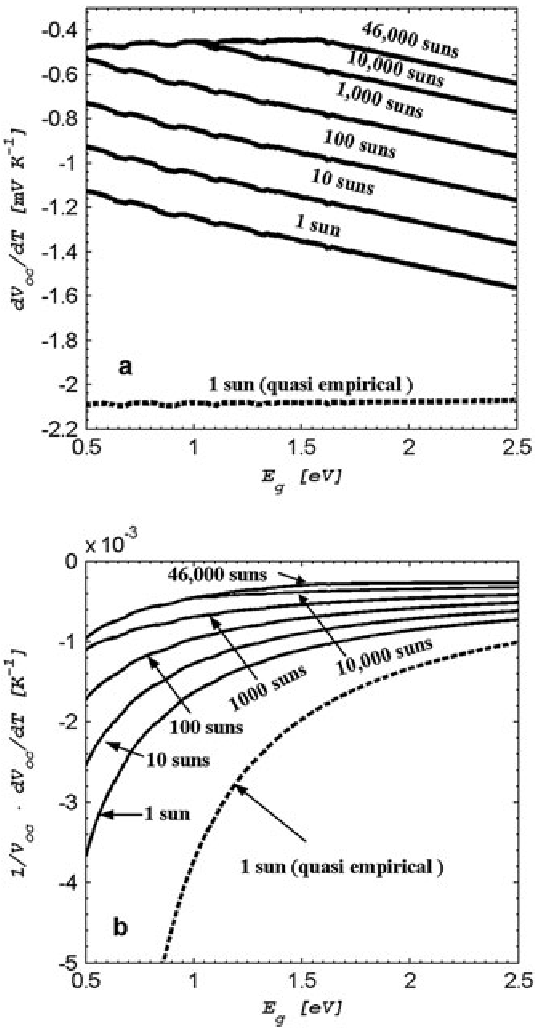

Figure 3. The temperature dependence of V_{oc} as a function of E_g for varying flux concentration. (a) dV_{oc}/dT. (b) $d\ln(V_{oc})/dT$. Solid curves indicate the radiative limit. The dashed curve is for the quasi-empirical model. For low-E_g materials at ultra-high irradiance, the curves coalesce because at such high carrier injection levels V_{oc} approaches E_g/q and hence ceases to increase with irradiance. The range of flux concentration is prompted by concentrator solar cell experiments having been reported up to ~10,000 suns, with 46,000 suns being the thermodynamic limit for concentration in air.

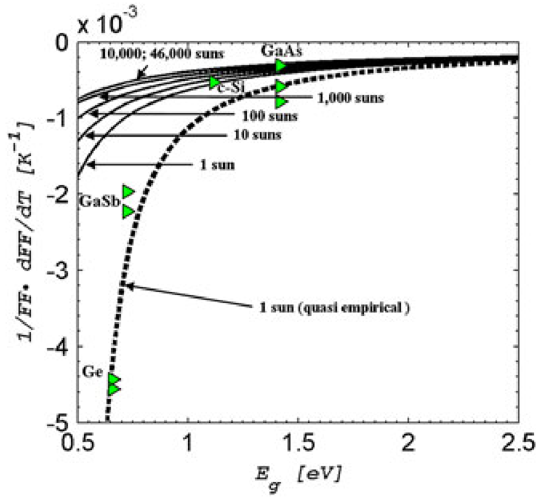

Figure 4. $d\ln(FF)/dT$ as a function of E_g for different concentration levels. Solid curves denote the radiative limit. The dashed curve is for the quasi-empirical model. Solid triangles represent measured one-sun temperature coefficients for the materials listed in Figure 1 [6,24].

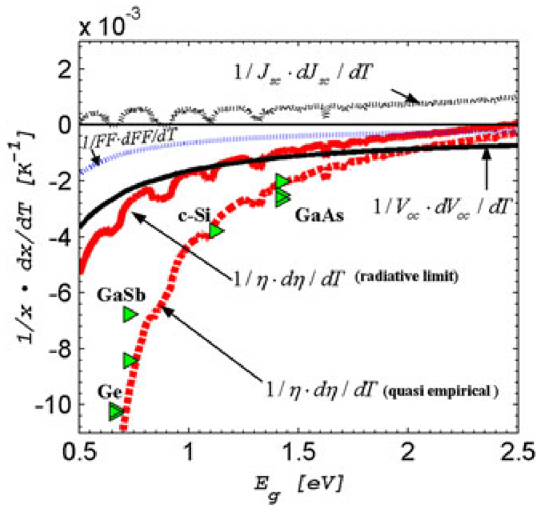

Figure 5. The relative temperature coefficients of J_{sc}, V_{oc}, FF, and η at one sun. Solid curves indicate the radiative limit. For clarity, the quasi-empirical model prediction is shown only for η (dashed curve). Solid triangles denote measured $d\ln(\eta)/dT$ at one sun for assorted solar cell materials [6,24].

Increased irradiance mitigates the efficiency penalty for cell heating for all bandgaps (Figure 6). In the radiative limit, there is a transition from negative to positive temperature coefficient, favoring higher bandgaps.

3.5. Multi-junction cells

We calculated the relative temperature coefficients of V_{oc} and J_{sc} for three different commercial triple-junction cell architectures under the ideality assumptions noted previously. (Attention has been restricted to three-junction cells as they represent the state-of-the-art of photovoltaic technology for which there are published experimental results against which to compare. The method depicted here can be extended to four and five-junction cells at such time as commercial devices and measurements thereon become available.) The first two structures—which have achieved efficiencies exceeding 41% under several hundred suns [25,26]—have Ge as their lowest sub-cell: (A) $Ga_{0.49}In_{0.51}P/Ga_{0.99}In_{0.01}As/Ge$ with respective bandgaps of 1.86/1.41/0.66 eV and (B) $Ga_{0.35}In_{0.65}P/Ga_{0.83}In_{0.17}As/Ge$ with 1.67/1.18/0.66 eV. The third structure (C)—designed

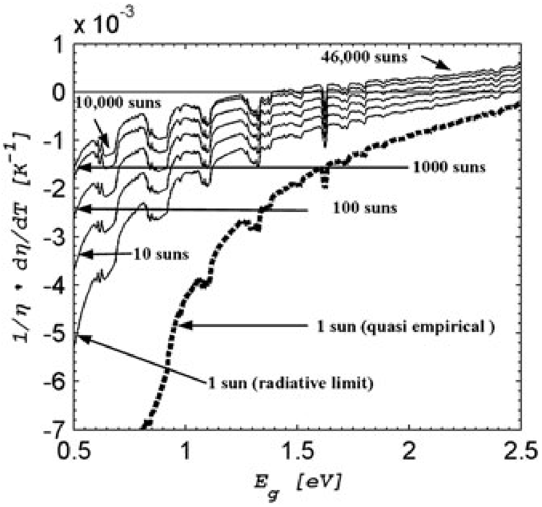

Figure 6. Calculated dln(η)/dT as a function of E_g for different concentration levels. Solid curves are for the radiative limit. For clarity and comparison, the quasi-empirical result is presented only at one sun (dashed curve).

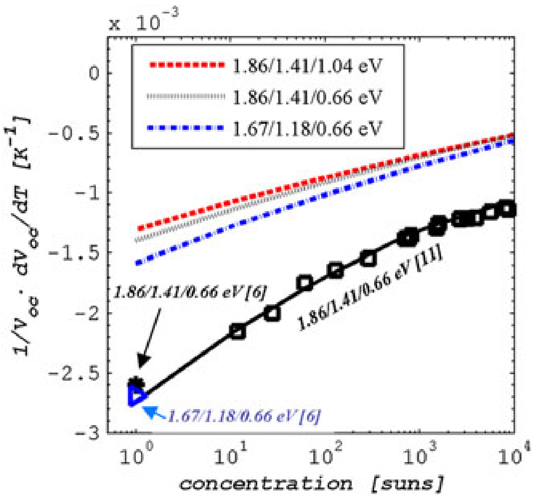

Figure 7. The relative temperature coefficient of V_{oc} for 3 distinct triple-junction cells as a function of concentration (semi-log plot). Dashed curves: the fundamental lower bound for |dln(V_{oc})/dT| of the radiative limit. Solid curve: calculated values according to Eq. 12, where the input information comprises measured values of V_{oc} and dV_{oc}/dT at 11 suns (the lowest irradiance at which measurements in [12] were performed) and $n(X)$ (with $n = 4.2$ for $X \leq 800$ and $n = 3$ for $X > 800$). The symbols indicate data for similar structures [6,12].

for potentially higher efficiency—has bandgaps of 1.86/1.41/1.04 eV, with a ~1 eV sub-cell (e.g., GaInNAs) replacing Ge [27].

Because the middle sub-cell is current-limiting, the temperature coefficient of J_{sc} is determined by the two upper junctions (Eq. 3). Hence, dJ_{sc}/dT is estimated as 0.0066 mA/(cm^2−K) for structures (A) and (C), and as 0.0079 mA/(cm^2−K) for (B). dln(J_{sc})/dT was calculated to be 0.00049 for (A) and (C), and 0.00047 K^{-1} for (B)—figures in accordance with experimental data [10,12].

The calculated effect of irradiance on the temperature coefficient of V_{oc} is illustrated in Figure 7 and is compared with available data. As expected from Eqs. 5, 7 and 10, |dln(V_{oc})/dT| decreases logarithmically and non-negligibly with concentration (confirmed by corresponding data). In addition, at fixed irradiance, lower-magnitude temperature coefficients were calculated for higher-E_g structures, demonstrating an additional potential advantage of choosing a ~1.0 eV bandgap sub-cell instead of the traditional Ge. The measured magnitude of dln(V_{oc})/dT is ~1.9–2.0 times larger than the lower bound of the radiative limit, for all values of flux concentration. Equation 12 again offers good agreement with corresponding experimental results.

4. SUMMARY

The contributions of J_{sc}, V_{oc}, and FF to the temperature dependence of η were investigated analytically, as a function of E_g and flux concentration, for single and multi-junction concentrator solar cells, both (i) in the radiative limit, for which fundamental bounds can be established and (ii) with a quasi-empirical model that affords favorable comparisons to available data.

Although the relative temperature coefficient of J_{sc} increases with E_g and does not change with concentration, the magnitudes of the relative temperature coefficients of V_{oc} and FF decrease with concentration (logarithmically) and with E_g. Indeed, for low-E_g materials under low concentration, the temperature coefficient of η is dominated by V_{oc}. However, for high-E_g materials or at elevated concentration, dln(J_{sc})/dT is comparable to (or even larger in magnitude than) dln(V_{oc})/dT and ceases to play merely a secondary role.

The efficiency penalty for cell heating decreases logarithmically with irradiance, and in principle, the temperature coefficient of η (but not that of V_{oc} or FF) could become positive in the radiative limit at adequately high irradiance and bandgap. In reality, however (i.e., for realistic cell properties, bandgaps, and irradiance levels), dln(η)/dT will remain negative. Nonetheless, the reduction in the magnitude of the negative dln(η)/dT as irradiance increases eases the burden on concentrator photovoltaic heat rejection systems (for a specified degree of cell heating).

The results for multi-junction cells follow the same trends as for single-junction cells: a lower heating penalty for cells that operate at high concentration and for cells comprising high-E_g materials. The calculated magnitude of the temperature coefficient of V_{oc} decreased by ~60% when irradiance increased from 1 to 10^4 suns, in agreement with available data. For such cells, a method for determining d$V_{oc}(X)$/dT from a measurement of dV_{oc}/dT and $n(X)$ has been demonstrated and compared favorably against experimental data [12].

Prog. Photovolt: Res. Appl. 2013; 21:1087–1094 © 2012 John Wiley & Sons, Ltd.
DOI: 10.1002/pip

The two models complement one another. The radiative limit, when applied to V_{oc} (the dominant parameter for most cells at one sun), yields a lower bound for the magnitude of its absolute and relative temperature coefficients. Compared with the available data, the results generated using the quasi-empirical approach furnish a satisfactory prediction for the temperature coefficients of V_{oc}, FF, and η.

ACKNOWLEDGEMENT

Avi Braun gratefully acknowledges the generous support of the Adams Fellowship of the Israeli Academy of Arts and Sciences.

REFERENCES

1. Wysocki JJ, Rappaport P. Effect of temperature on photovoltaic solar energy conversion. *Journal of Applied Physics* 1960; **31**: 571–578. DOI : 10.1063/1.1735630
2. Fan JCC. Theoretical temperature dependence of solar cell parameters. *Solar Cells* 1986; **17**: 309–315. DOI: 10.1016/0379-6787(86)90020-7
3. Weinberg I, Swartz CK, Hart RE, Ghandhi SK, Borrego JM, Parat KK, Yamaguchi M. Comparative radiation resistance, temperature dependence and performance of diffused junction indium phosphide solar cells. *Solar Cells* 1987; **22**: 113–124. DOI: 10.1016/0379-6787(87)90051-2
4. Yoon S, Garboushian V. Reduced temperature dependence of high-concentration photovoltaic solar cell open-circuit voltage (V_{oc}) at high concentration levels. *Proceedings of the IEEE 24th Photovoltaic Specialists Conference* 1994; **2**: 1500–1504. DOI: 10.1109/WCPEC.1994.520235
5. Green MA. General temperature dependence of solar cell performance and implications for device modeling. *Progress in Photovoltaics* 2003; **11**: 333–340. DOI: 10.1002/pip.496
6. Siefer G, Abbott P, Baur C, Schlegl T, Bett AW. Determination of the temperature coefficients of various III–V solar cells. *Proceedings of the 20th European Photovoltaic Solar Energy Conference*, WIP Renewable Energies, Munich, Barcelona, 2005; 495–498.
7. Nishioka K, Takamoto T, Agui T, Kaneiwa M, Uraoka Y, Fuyuki T. Annual output estimation of concentrator photovoltaic systems using high-efficiency InGaP/InGaAs/Ge triple-junction solar cells based on experimental solar cell's characteristics and field-test meteorological data. *Solar Energy Materials and Solar Cells* 2006; **90**: 57–67. DOI: 10.1016/j.solmat.2005.01.011
8. Kinsey GS, Hebert P, Barbour KE, Krut DD, Cotal HL, Sherif RA. Concentrator multijunction solar cell characteristics under variable intensity and temperature. *Progress in Photovoltaics* 2008; **16**: 503–508. DOI: 10.1002/pip.834
9. Friedman DJ. Modelling of tandem cell temperature coefficients. *Proceedings of the 25th IEEE Photovoltaic Specialists Conference*, IEEE, 1996; 89–92. DOI: 10.1109/PVSC.1996.563954
10. Kinsey GS, Edmondson KM. Spectral response and energy output of concentrator multi-junction solar cells. *Progress in Photovoltaics* 2009; **17**: 279–288. DOI: 10.1002/pip.875
11. Aiken D, Stan M, Murray C, Sharps P, Hills J, Clevenger B. Temperature dependent spectral response measurements for III–V multi-junction solar cells. *Proceedings of the 29th IEEE Photovoltaic Specialists Conference*, 2002; 828–831. DOI: 10.1109/PVSC.2002.1190704
12. Braun A, Hirsch B, Vossier A, Katz EA, Gordon JM. Temperature dynamics of multi-junction concentrator solar cells up to ultra-high irradiance. *Progress in Photovoltaics* 2012; in press. DOI: 10.1002/pip.1179
13. Katz EA, Gordon JM, Tassew W, Feuermann D. Photovoltaic characterization of concentrator solar cells by localized irradiation. *Journal of Applied Physics* 2006; **100**: 044514–044518. DOI: 10.1063/1.2266161
14. Parrott JE. Self-consistent detailed balance treatment of the solar cell. *IEE Proceedings-J Optoelectronics* 1986; **133**: 314–318. DOI: 10.1049/ip-j:19860054
15. Sze SM, Ng KK. Physics of Semiconductor Devices (3rd edn). Wiley-Interscience: Hoboken, NJ, 2007.
16. Vurgaftman I, Meyer JR, Ram-Mohan LR. Band parameters for III–V compound semiconductors and their alloys. *Journal of Applied Physics* 2001; **89**: 5815–5875. DOI: 10.1063/1.1368156
17. Kasap SO, Capper P. Springer Handbook of Electronic and Photonic Materials. Springer Verlag: New York, 2006.
18. Varshni, YP. Temperature dependence of the energy gap in semiconductors. *Physica* 1967; **34**: 149–154. DOI: 10.1016/0031-8914(67)90062-6
19. Braun A, Szabó N, Schwarzburg K, Hannappel T, Katz EA, Gordon JM. Current-limiting behavior in multi-junction solar cells. *Applied Physics Letters* 2011; **98**: 223506. DOI: 10.1063/1.3596444
20. Baruch P, De Vos A, Landsberg PT, Parrott JE. On some thermodynamic aspects of photovoltaic solar energy conversion. *Solar Energy Materials and Solar Cells* 1995; **36**: 201–222. DOI: 10.1016/0927-0248(95)80004-2
21. King RR, Sherif R, Kinsey GS, Kurtz S, Fetzer CM, Edmondson KM, Law DC, Cotal HL, Krut DD, Ermer JH, Karam NH. Bandgap engineering in

high-efficiency multi-junction concentrator cells. *International Conference on Solar Concentrators for the Generation of Electricity or Hydrogen*, Scottsdale, AZ, NREL/CD-520-38172, 2005.
22. Algora C. The importance of the very high concentration in third generation solar cells. In Next Generation Photovoltaics, High Efficiency Through Full Spectrum Utilization Ch 6, Martí A, Luque A (eds). Institute of Physics: Bristol, UK, 2004; 108–139.
23. Wurfel P. Physics of Solar Cells: From Basic Principles to Advanced Concepts (2nd edn). Wiley-VCH: Weinheim, 2009.
24. SunPower Corp. 1414 Harbour Way, South Richmond, CA 94804. E19/240 Solar Panel. Technical Document #001-65327, 2010.
25. Guter W, Schöne J, Philipps SP, Steiner M, Siefer G, Wekkeli A, Welser E, Oliva E, Bett AW, Dimroth F. Current-matched triple-junction solar cell reaching 41.1% conversion efficiency under concentrated sunlight. *Applied Physics Letters* 2009; **94**: 223504. DOI: 10.1063/1.3148341
26. King RR, Law DC, Edmondson KM, Fetzer CM, Kinsey GS, Yoon H, Sherif RA, Karam NH. 40% efficient metamorphic GaInP/GaInAs/Ge multi-junction solar cells. *Applied Physics Letters* 2007; **90**: 183516. DOI: 10.1063/1.2734507
27. Kurtz SR, Allerman AA, Jones ED, Gee JM, Banas JJ, Hammons BE. InGaAsN solar cells with 1.0 eV band gap, lattice matched to GaAs. *Applied Physics Letters* 1999; **74**: 729–731. DOI: 10.1063/1.123105